

Interference Localisation Methods using Direct Position Determination Concept

Joon Wayn Cheong

School of Electrical Engineering and Telecommunications
UNSW Sydney, Australia
Ph: +61 (2) 93856702 Email: cjwayn@unsw.edu.au

Andrew G. Dempster

School of Electrical Engineering and Telecommunications
UNSW Sydney, Australia
Ph: +61 (2) 93856890 Email: a.dempster@unsw.edu.au

ABSTRACT

GNSS users are vulnerable to in-band jamming and/or spoofing from terrestrial sources. This is especially critical to safety-of-life applications that relies heavily on GNSS signals to provide positional information. Prime examples of this include passenger airliners, autonomous self-driving vehicles and military equipment. Providing a situational awareness of the status of the GNSS signals in such environments (e.g. an airport) is crucial to prevent the GNSS-reliant systems from failing and to provide the jamming source's positional information for law enforcement to rapidly disarm the interference source.

This paper focuses on recent advancement in the detection and localisation of multiple interferers using phased array antennas as sensors. Various perspectives of the Direct Position Determination concept are presented and compared and its results presented.

KEYWORDS: Interference, Localisation, Jamming, Spoofing, Phased Array, Signal Processing

1. INTRODUCTION

Authentic GNSS signals transmitted from space are inherently weak, leaving GNSS users prone to interference from intentional or unintentional strong terrestrial transmitters. This leaves safety-critical services such as aviation, maritime and military operations that depend on GNSS highly vulnerable. This is exacerbated by the highly available and cost-effective Personal Privacy Devices (PPD) that are effectively GNSS jammers. The aim of this paper is to analyse and develop a highly sophisticated method to geo-locate jammers using a network of sensors deployed around a highly valuable facility such as an airport. Once a jammer has been identified, the geolocation information will assist relevant enforcement agencies to disarm the jammer, capture the perpetrator of an intentional jamming, and/or provide useful evidence for

prosecution.

1.1 Jammer Types

Jammers effective against GNSS users can be broadly categorised into two categories: narrowband and wideband. Narrowband jammers are easy to produce and can be easily detected and especially effective against high precision GNSS receivers. The signals categorised as narrowband are Continuous Wave (CW), Single Sideband (SSB), and Amplitude modulation (AM), Narrowband Frequency Modulation (NBFM), etc. This type of jammer can be detected using a Phased Array Antenna (PAA) system setup at a sensor site. A PAA can identify the presence and the angle of arrival (AoA) of the narrowband jammer signal received at the sensor site.

Wideband jammers include signals generated using Swept Frequency Modulation (Swept FM) and pseudorandom noise (PRN). This type of signals can also be detected using a PAA system but more importantly, cross-correlation and autocorrelation techniques can be used to identify these wideband jammers. This is a technique that cannot be applied for narrowband jammer signals as the autocorrelation function of a narrowband jammer signal does not yield a distinct peak (i.e. does not approximate a dirac delta function). Finally, the cross-correlation technique applied to a pair of widely separated sensor sites can be used to identify the Time Difference of Arrival (TDoA) of the wideband signal arriving at both nodes. Also it is important to note that unlike narrowband signals, TDoA observations can be obtained using as few as one antenna element per sensor site.

1.2 Conventional Geolocation Methods

Conventionally, jammer signals are first detected on individual AoA and TDoA domains (Van Trees, 2002) and then geolocated by solving a set of linear and nonlinear equations. In a simplified two-dimensional space, these equations represents the straight lines formed by a given set of AoA observations and the hyperbolic lines formed a set of TDoA observations. The geolocation is done by identifying intersections of observations from all sensor sites. (Bishop, Fidan, Doğançay, Anderson, & Pathirana, 2008) This conventional geolocation method is also widely known as the two-step method.

Under multiple jammer situations, there will be more than one intersection of lines and under realistic circumstances some observations may be outliers. To make things worse, certain scenarios may result in two or more jammers to observe the same AoA and/or TDoA values. These situations poses significant difficulties to correctly geolocate using AoA and TDoA observations and subsequent methods employed to overcome these issues are workarounds that are imperfect.

It is thus the intention of this paper to analyse and develop a technique that perform geolocalisation directly on the signal domain. This bypasses the intermediate step of estimating TDoA and AoA observations.

2. Background

This paper will focus on the concept of Direct Position Determination (DPD) (Weiss, 2004). This concept performs simultaneous signal processing on signal streams from all antenna elements and all sensor sites. DPD interacts directly with the signal streams according to the

architecture described in Fig 1. It aims to:

- Combine signal energy from all antenna elements in the network
- Avoid sub-optimality associated with intermediate estimation steps such as AoA estimation and TDoA estimation.
- Avoid ambiguity issues associated with resolving multiple line intersections.
- Provide higher positioning accuracy than conventional two-step methods.

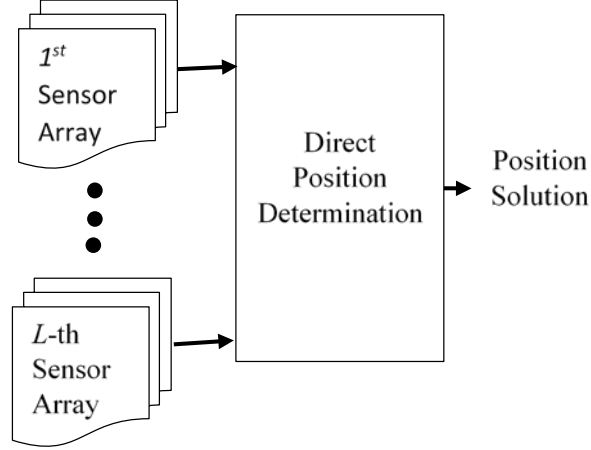


Figure 1. Architecture of the Direct Position Determination (DPD) concept.

2.1 Signal Model

Consider Q interference sources transmitting wideband signals of unknown waveform that can be observed by L sensor stations. Each sensor station is equipped with an M -element phased array.

The $M \times 1$ vector of complex baseband signals observed at the l -th array can be modelled as:

$$\mathbf{r}_l(t) = \sum_{q=1}^Q \alpha_{l,q} \mathbf{a}_l(\mathbf{p}_q) s_q(t - \tau_{l,q}(\mathbf{p}_q)) + \mathbf{n}_l(t) = \mathbf{A}_l \mathbf{\Omega}_l \mathbf{s}_l(t) + \mathbf{n}_l(t) \dots \dots \dots (1)$$

Where $\alpha_{l,q}$ is the complex scalar representing the path attenuation coefficient for sensor l and jammer/source q , $\mathbf{a}_{l,q}(\mathbf{p})$ is the $M \times 1$ vector of complex coefficients representing the antenna's steering vector in response to the source at location \mathbf{p}_q , $s(t - \tau_l(\mathbf{p}_q))$ is the complex baseband representation of the transmitted signal waveform delayed by $\tau_l(\mathbf{p}_q)$ and $\mathbf{n}_l(t)$ is the $M \times 1$ vector of complex Gaussian white noise. Therefore, the matrix representations used are $\mathbf{A}_l = [\mathbf{a}_l(\mathbf{p}_1) \dots \mathbf{a}_l(\mathbf{p}_Q)]$, $\mathbf{s}_l(t) = [s_1(t - \tau_{l,1}(\mathbf{p}_1)) \dots s_Q(t - \tau_{l,Q}(\mathbf{p}_Q))]$, $\mathbf{\Omega}_l = (\delta_{j,q} \alpha_{l,q})_{1 \leq q \leq Q}$.

2.2 Existing Approaches

In existing literatures, geo-localising an interference source is done for wideband sources by splitting the signal into multiple narrowband signals. Methods adopting this model is found in DPD (Tirer & Weiss, 2017), LOST (Bosse, Ferreol, & Larzabal, 2013), LOST-FIND (Delestre, Ferreol, & Larzabal, 2015) and HR-DPD (Tzafri & Weiss, 2016). The signal model adopted for this type of algorithms typically resemble:

$$\mathbf{r}_\ell(j, k) = \sum_{q=1}^Q b_{\ell q} \mathbf{a}_\ell(\mathbf{p}_q) s_q(j, k) e^{-i\omega_j [\tau_\ell(\mathbf{p}_q) + t_q^{(0)}]} + \mathbf{n}_\ell(j, k),$$

$$j = 1, 2, \dots, J; k = 1, 2, \dots, K, \dots\dots\dots(2)$$

where,

$$\bar{s}_q(j, k) \triangleq s_q(j, k) e^{-i\omega_j t_q^{(0)}},$$

$$\bar{\mathbf{a}}_\ell(j, \mathbf{p}_q, b_{\ell q}) \triangleq b_{\ell q} \mathbf{a}_\ell(\mathbf{p}_q) e^{-i\omega_j \tau_\ell(\mathbf{p}_q)}$$

In the author's opinion, this form of narrowband decomposition are combining the various frequency components of a wideband signal in a way that eliminates the TDOA information embedded within $s(t - \tau_l(\mathbf{p}))$. The narrowband decomposition does not exploit the cross-correlation properties of wideband signals.

A method that doesn't employ frequency splitting is TARGET (Delestre, Ferreol, Larzabal, & Germond, 2015). TARGET uses cross-correlation between signals from all nodes as its input for processing. For completeness, we briefly describe the TARGET algorithm here to draw comparison to our proposed method in the next section.

2.3 TARGET

In TARGET, we first consider pairs of sensor arrays. We first concatenate two $\mathbf{r}_l(t)$ vectors from station i and j to form the observed signal vector $\mathbf{x}_{i,j}(t, \tau)$

$$\mathbf{x}_{i,j}(t, \tau) = [\mathbf{r}_i^T(t) \quad \mathbf{r}_j^T(t + \tau)]^T \dots\dots\dots(3)$$

Then, we can describe (2) based on (1) as

$$\mathbf{x}_{i,j}(t, \tau) = \sum_{q=1}^Q \mathbf{U}(\mathbf{p}_q) \mathbf{s}_q(t, \tau) + \mathbf{n}_l(t, \tau) \dots\dots\dots(4)$$

$$\mathbf{U}(\mathbf{p}_q) = \begin{bmatrix} \alpha_{i,q} \mathbf{a}_i(\mathbf{p}_q) & 0 \\ 0 & \alpha_{j,q} \mathbf{a}_j(\mathbf{p}_q) \end{bmatrix}$$

$$\mathbf{s}_q(t, \tau) = \begin{bmatrix} s_q(t - \tau_{i,q}(\mathbf{p}_q)) \\ s_q(t - \tau_{j,q}(\mathbf{p}_q) + \tau) \end{bmatrix}$$

The covariance matrix of $\mathbf{x}_{i,j}(t)$ expressed as $\mathbf{R}_x(\tau)$ can be shown as

$$\mathbf{R}_x(\tau) = \mathbb{E}_t \left(\mathbf{x}_{i,j}(t, \tau) \mathbf{x}_{i,j}^H(t, \tau) \right)$$

$$\mathbf{R}_x(\tau) = \begin{bmatrix} \mathbf{R}_{ii} & \mathbf{R}_{ij}(\tau) \\ \mathbf{R}_{ji}(-\tau) & \mathbf{R}_{jj} \end{bmatrix} + \mathbf{R}_n \dots \dots \dots (5)$$

where $\mathbf{R}_{ii} = \sum_q \mathbf{a}_i(\mathbf{p}_q) \Lambda_{ii} \mathbf{a}_i^H(\mathbf{p}_q) \alpha_{i,q}^2$ and $\mathbf{R}_{ij}(\tau) = \sum_q \alpha_{i,q} \mathbf{a}_i(\mathbf{p}_q) \Lambda_{ij}(\tau) \mathbf{a}_j^H(\mathbf{p}_q) \alpha_{j,q}^*$. The transmitted signals' autocorrelation and cross correlation functions are defined as $\Lambda_{ii} = \mathbb{E}_t \left(s_i(t) s_i^H(t) \right)$ and $\Lambda_{ij}(\tau) = \mathbb{E}_t \left(s_i(t) s_j^H(t + \tau) \right)$ respectively. Note that $R_{ji}(\tau) = R_{ij}^H(-\tau)$.

We further define the matrix $\mathbf{G}_{ij}(\tau)$ as

$$\mathbf{G}_{ij}(\tau_{ij}) = \mathbf{I}_M - \mathbf{R}_{ii}^+ \mathbf{R}_{ij}(-\tau_{ij}) \mathbf{R}_{jj}^+ \mathbf{R}_{ji}(\tau_{ij})$$

Where,

$$\mathbf{R}_{ii}^+ = \mathbf{\Pi}_i \mathbf{\Sigma}^{-1} \mathbf{\Pi}_i^H \quad \mathbf{R}_{ii} = \mathbf{\Pi}_i \mathbf{\Sigma} \mathbf{\Pi}_i^H$$

The $Q \times Q$ diagonal matrix $\mathbf{\Sigma}^{-1}$ is the inverse of Q largest eigenvalues of \mathbf{R}_{ii} and its corresponding Q eigenvectors is represented by the $M \times Q$ matrix $\mathbf{\Pi}_i$. τ_{ij} is defined as the TDoA speculated between node i and j defined as $\tau_{ij} = \tau_j - \tau_i$. Then we can finally jointly estimate the AOA for sensor site i $\hat{\boldsymbol{\theta}}_i$ and TDoA between node i and j $\hat{\boldsymbol{\tau}}_{ij}$ from the following cost function derived from the Rayleigh quotient

$$(\hat{\boldsymbol{\theta}}_i, \hat{\boldsymbol{\tau}}_{ij}) = \underset{\boldsymbol{\theta}_i, \tau_{ij}}{\operatorname{argmin}} \frac{\mathbf{a}_i^H(\boldsymbol{\theta}_i) \mathbf{G}_{ij}(\tau_{ij}) \mathbf{a}_i(\boldsymbol{\theta}_i)}{\mathbf{a}_i^H(\boldsymbol{\theta}_i) \mathbf{a}_i(\boldsymbol{\theta}_i)} \dots \dots \dots (6)$$

3. A Geo-localisation Algorithm for TARGET

A method for geolocation was not stated explicitly in the original paper (Delestre, Ferreol, Larzabal, et al., 2015). Hence, the following derivations here are used for position estimation. The proposed algorithm here estimates the source location using the Rayleigh quotient as

$$\hat{\mathbf{p}}_q = \underset{\mathbf{p} \in \mathbf{P}}{\operatorname{argmin}} \frac{1}{L(L-1)} \sum_{i \neq j} J_{T,ij}(\mathbf{p}_q) \quad \forall i, j \in [1, L] \dots \dots \dots (7)$$

where

$$J_{T,ij}(\mathbf{p}_q) = \frac{\mathbf{a}_i^H(\mathbf{p}_q) \mathbf{G}_{ij}(\tau(\mathbf{p}_q)) \mathbf{a}_i(\mathbf{p}_q)}{\mathbf{a}_i^H(\mathbf{p}_q) \mathbf{a}_i(\mathbf{p}_q)}$$

An example of the result of the sum of $J_{T,ij}(\mathbf{p}_q)$ is shown in Fig 2. This plot is based on a scenario with a single source at $x = -90\text{m}$ $y = -475\text{m}$ and three sensor arrays at $x = 0\text{m}$, $y = 0\text{m}$, $x = 0\text{m}$, $y = -725\text{m}$ and $x = -380\text{m}$, $y = 0\text{m}$. The algorithm is able to produce a highly distinct and sharp global minimum at the correct source location.

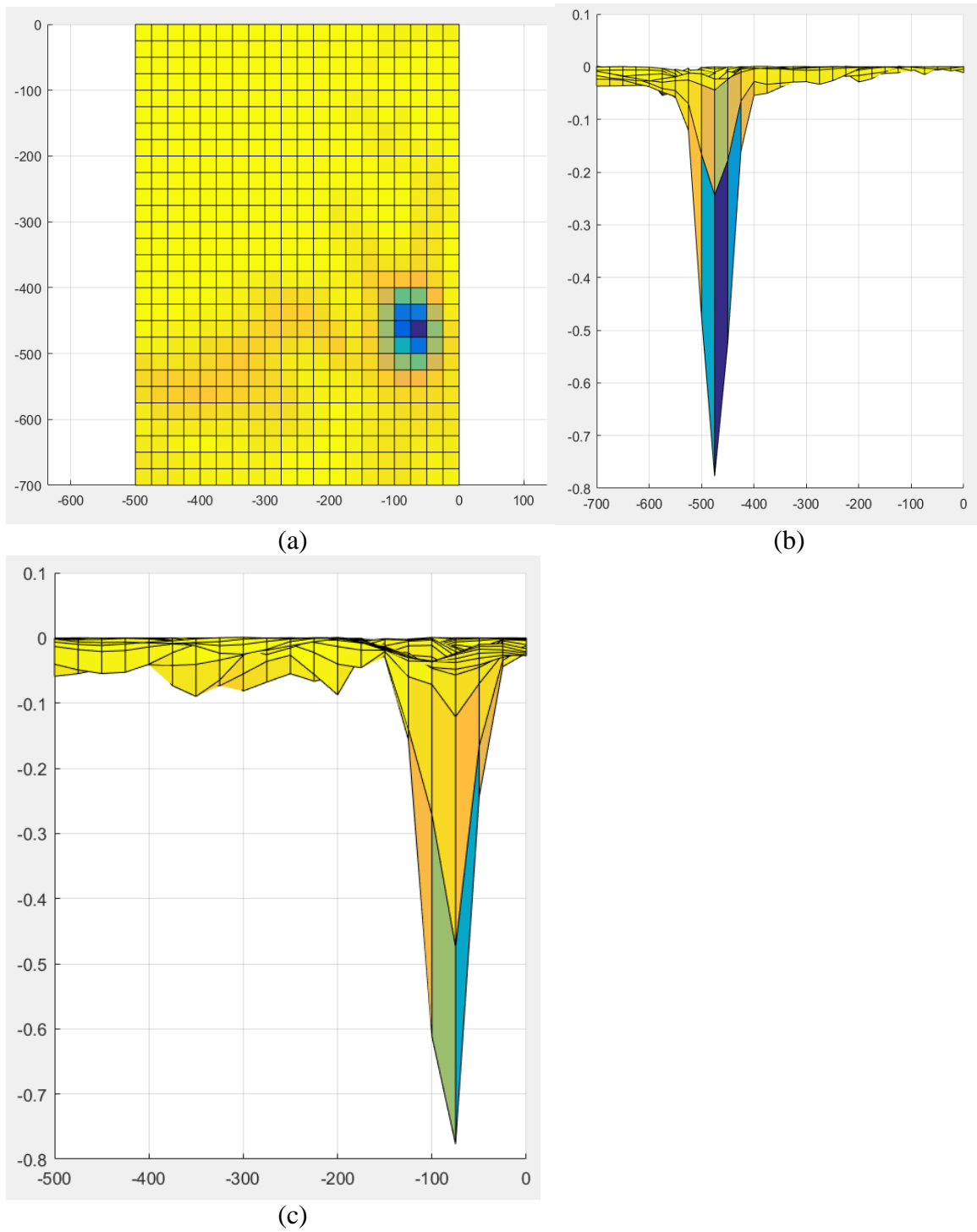


Figure 2. (a) X-Y, (b) Y-Z and (c) X-Z domain plot of the sum of cost functions (z-axis) vs position space (x,y-axis)

3.1 Limitations of TARGET

Like most subspace-based techniques, TARGET assumes that the number of jammers/sources Q to be known a priori. The lack of such knowledge will produce multiple false local minima and/or significantly higher noise floor.

The number of detectable jammer/sources are limited to the smallest number of antenna element of the sensor network (Delestre, Ferreol, Larzabal, et al., 2015). This is due to the eigen-decomposition performed at the array level instead of the network level. This significantly limits the applicability of this algorithm in multiple jammer/sources scenario, especially when the jammer is far away (i.e. the received signal is weak) and GNSS signals start to appear as significant peaks in the spectrum.

TARGET does not combine the signal energy arriving at individual sensor site. It only exploits the spatial diversity of the arriving signals to perform geo-localisation. In a network with a large number of sensor sites (i.e. $L \gg 1$), the signal-to-noise ratio advantage is substantial if an algorithm does adopt the concept of signal combining. This showcases the lack of sensitivity of TARGET.

4. Simulation Results

In this section, we simulate a scenario based on the signal model described by (1). Simulated signals for each jammer/source take the form of a continuous pseudorandom noise with 10MHz bandwidth on both In-phase and Quadrature phase channels.

There are a total of four PAAs in the network, each employing an identical eight element Uniform Circular Array (UCA). The radius of each array is 1.5λ where $\lambda = 1/f_c$. The sampling frequency for the baseband equivalent signal stream for each antenna element is 20MHz. The modelled baseband equivalent signal is based on the center frequency $f_c = 1575.42\text{MHz}$, the nominal frequency for GPS L1 signals. For the following subsections, the jammer/source signals arriving at the antenna elements are modelled based on a signal-to-noise ratio of -10dB.

4.1 Scenario 1: Multiple Jammers

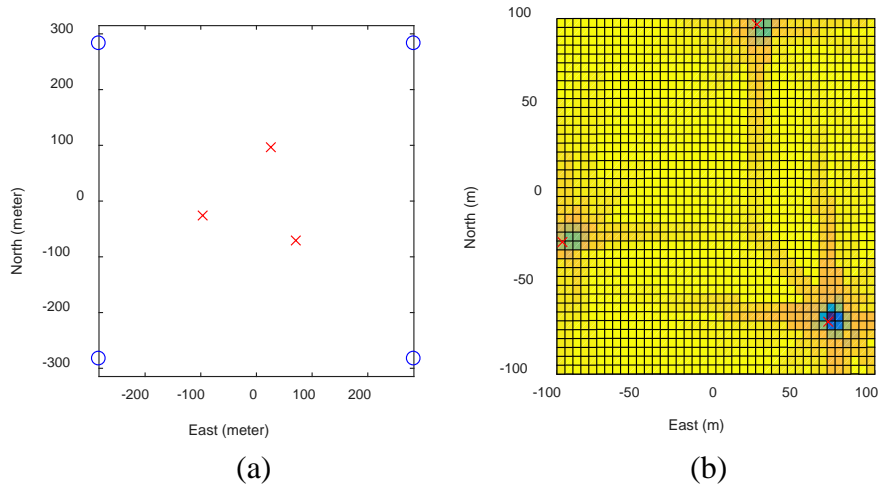


Figure 3. (a) Scenario map with three jammers/sources indicated by red crosses and four UCA sensor arrays denoted by blue circles. (b) TARGET cost function over the two dimensional position domain.

In this scenario in Fig 3(a), we consider a largely benign situation where most algorithms including the conventional two-step algorithms would perform well. The three source signals impinging each sensor site would satisfy the $Q < M$ requirement of TARGET and result in successful eigen-decomposition of \mathbf{R}_{ii} . Successful geo-localisation is seen in Fig 3(b).

4.2 Scenario 2: Heavy Background GNSS

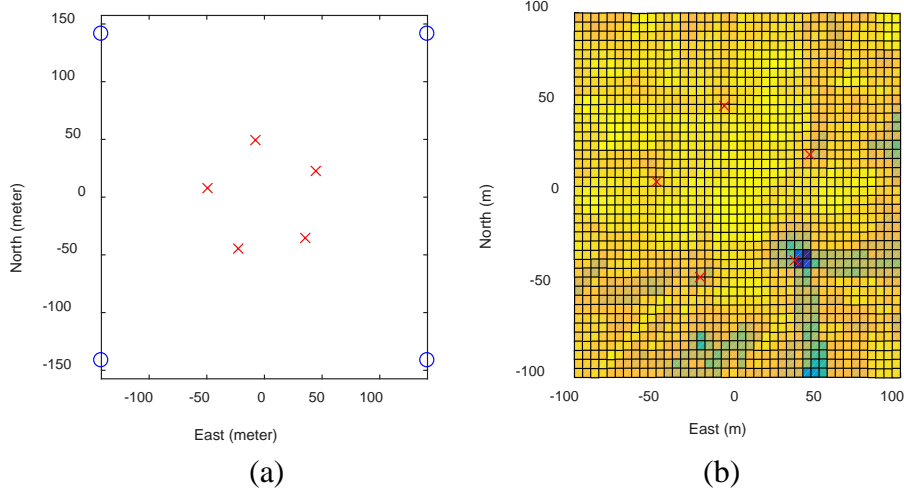


Figure 4. (a) Scenario with five jammers/sources indicated by red crosses and four UCA sensor arrays denoted by blue circles and eight GNSS signal sources not shown here. (b) TARGET cost function over the two dimensional position domain

In the case where a source/jammer signal is weak, the effect of background GNSS signals starts to become significant. We consider a case where eight GNSS sources distributed evenly over the horizon are impinging the antennas at a signal strength 20dB weaker than the jammer signals would. The TARGET spatial spectrum as shown in Fig 4(b) indicates correct geo-localisation for one jammer/source and failure to geolocate four other jammers/sources given the sensor-jammer scenario in Fig 4(a).

This scenario is challenging for TARGET as the GNSS signals of substantial signal strengths starts to affect the representation of noise and jammer/source signals in \mathbf{R}_{ii} , resulting in a distorted eigenvector.

4.3 Scenario 3: Large Number of Sources

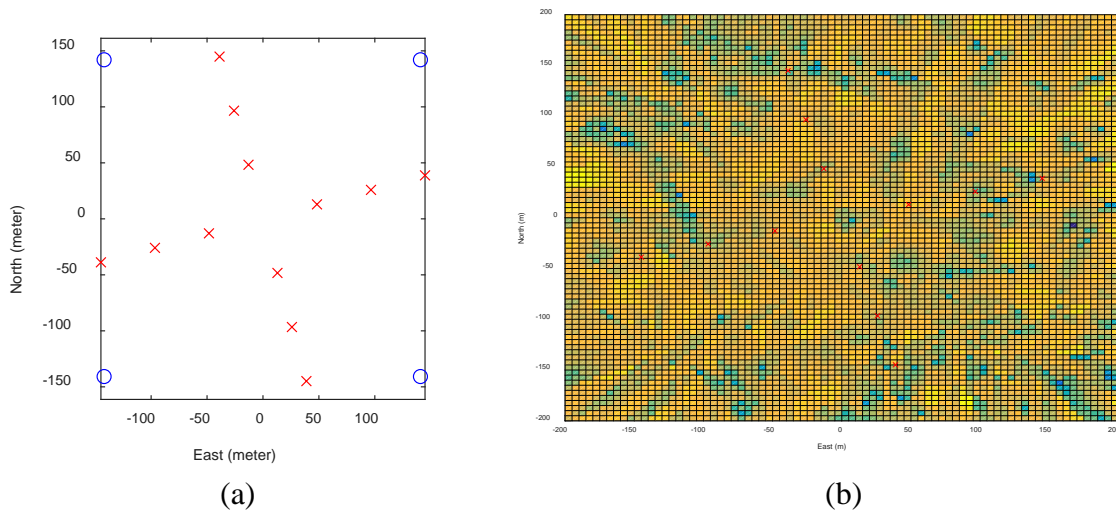


Figure 5. (a) Scenario with twelve jammers/sources indicated by red crosses and four UCA sensor arrays denoted by blue circles. (b) TARGET cost function over the two dimensional position domain

As described in section 3, TARGET becomes highly challenged when the number of sources exceed the number of antenna elements per sensor site (sensor array). The scenario here exemplifies this. As can be seen in Fig 5(b), the geolocation of any of the jammers/sources present has failed as indicated by the lack of distinct local minima or throughs.

5. Validation using Field Data

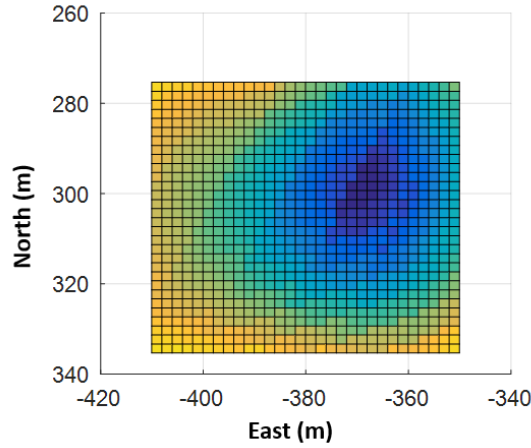


Figure 6. TARGET cost function over the two dimensional position domain using field data provided by GPSat Systems Australia Pty Ltd

To validate our mathematical signal models, algorithm implementation and signal simulation system, we used a field data collected by GPSat Systems Australia Pty Ltd in Victoria, Australia to replace the simulated signal stream in our algorithms implemented for section 4. As can be seen, the global maximum of a single jammer/source at $x = -370\text{m}$, $y = 300\text{m}$ is distinctly and accurately identified and geo-located by TARGET.

6. Conclusion

This paper discussed the merits of Direct Position Determination (DPD) and compared it against various conventional geolocation techniques. While DPD is largely solved for narrowband systems, various approaches adopted by DPD for wideband signals has failed to take advantage of the cross-correlation characteristics of such wideband signals. TARGET is the first and only DPD approach to date that has tried to exploit this characteristic but the analysis shown in this paper has revealed and verified several limitations posed by this algorithm. It is the intention of this paper to spawn more sophisticated algorithms that circumvents these limitations.

ACKNOWLEDGEMENTS

The authors would like to thank Dr Ryan Thompson and Mr Graeme Hooper from GPSat Systems Australia Pty Ltd for providing field data of a GNSS jamming scenario. This work is funded by the Australia Research Council under ARC Linkage LP140100252.

REFERENCES

- Bishop, A. N., Fidan, B., Doğançay, K., Anderson, B. D. O., & Pathirana, P. N. (2008). Exploiting geometry for improved hybrid AOA/TDOA-based localization. *Signal Processing*, 88(7), 1775–1791. <https://doi.org/10.1016/j.sigpro.2008.01.015>
- Bosse, J., Ferreol, A., & Larzabal, P. (2013). A Spatio-Temporal array processing for passive localization of radio transmitters. *IEEE Transactions on Signal Processing*, 61(22), 5485–5494. <https://doi.org/10.1109/TSP.2013.2278515>
- Delestre, C., Ferreol, A., & Larzabal, P. (2015). LOST-FIND: A spectral-space-time direct blind geolocalization algorithm. *ICASSP, IEEE International Conference on Acoustics, Speech and Signal Processing - Proceedings, 2015–August*, 2619–2623. <https://doi.org/10.1109/ICASSP.2015.7178445>
- Delestre, C., Ferreol, A., Larzabal, P., & Germond, C. (2015). TARGET: A direct AOA-TDOA estimation for blind broadband geolocalization. *2015 23rd European Signal Processing Conference, EUSIPCO 2015*, 2616–2620. <https://doi.org/10.1109/EUSIPCO.2015.7362858>
- Tirer, T., & Weiss, A. J. (2017). Performance Analysis of a High-Resolution Direct Position Determination Method. *IEEE Transactions on Signal Processing*, 65(3), 544–554. <https://doi.org/10.1109/TSP.2016.2621729>
- Tzafri, L., & Weiss, A. J. (2016). High-resolution direct position determination using MVDR. *IEEE Transactions on Wireless Communications*, 15(9), 6449–6461. <https://doi.org/10.1109/TWC.2016.2585116>
- Van Trees, H. L. (2002). *Optimum Array Processing* (1st ed.). Wiley-Interscience.
- Weiss, A. J. (2004, May). Direct position determination of narrowband radio frequency transmitters. *IEEE Signal Processing Letters*. <https://doi.org/10.1109/LSP.2004.826501>